Journal of the Korean Physical Society, Vol. 66, No. 5, March 2015, pp. 800∼805

Effect of Sintering Parameters on the Electrical and the Piezoelectric Properties of Double-calcined ($K_{0.48}Na_{0.48}Li_{0.04}$) ($Nb_{0.96}Sb_{0.04}$) O_3 Nanopowders

Roopam Gaur* and K. Chandramani Singh†
Department of Physics, Sri Venkateswara College, University of Delhi, New Delhi-110021, India

Radhapiyari Laishram‡
Solid State Physics Laboratory, Lucknow Road, Timarpur, Delhi - 110054, India

(Received 5 August 2014, in final form 13 November 2014)

The present work is an attempt towards understanding the effect of sintering parameters on the various morphological, electrical and piezoelectric properties of ($K_{0.48}Na_{0.48}Li_{0.04}$) ($Nb_{0.96}Sb_{0.04}$) O_3 (KNLNS) ceramics. We first synthesized the powder composition from various raw materials by using a conventional solid-state reaction method followed by high-energy ball milling. The powder sample was then sintered under various sintering conditions with temperatures ranging from 1050 °C to 1090 °C and durations from 2 h to 3 h. The ceramic samples so obtained were then characterized for various properties. The density was found to increase significantly within a narrow temperature range, but tended to decrease when the sintering temperature slightly exceeded the optimal one. Also, by merely reducing the duration of sintering from 3 h to 2 h while keeping the temperature constant, we observed an enhancement in the density of the ceramics by about 10% ∼ 20%. The room-temperature dielectric constant (ε_{RT}), the electromechanical coupling factor (k_p) and the piezoelectric charge constant (d_{33}) were found to vary with the sintering parameters. The study reveals the necessity for striking a strict balance between the sintering temperature and the sintering period in order to improve the microstructural, dielectric and piezoelectric properties of such a ceramic composition containing highly-volatile alkaline members.

PACS numbers: 77.84.-s, 77.90.+k
Keywords: Dielectric, Piezoelectric, Lead-free, KNN
DOI: 10.3938/jkps.66.800

I. INTRODUCTION

Ranking second in the list of prioritized hazardous substances issued by the U.S. ATSDR (Agency for Toxic Substances and Disease Registry) in 1999, lead is being phased out due to environmental concerns, safety issues, and its uncontrolled dispersion in the environment. The use of lead is most prominent in the electronics industry, which has been using lead zirconium titanate ($Pb(Ti,Zr)O_3$, PZT) as the chief piezoelectric material for past few decades due to its outstanding piezoelectric and dielectric properties. As PZT contains 60 wt% of lead, the RoHs (*Restriction of Hazardous Substances Directive*) and the WEEE (*Waste Electrical and Electronic Equipment Directive*) have announced intentions to eliminate PZT from the electronics industry at the earliest possible date. Various substituents have been thought of and worked upon in order to produce lead-free piezoceramics, but sodium potassium niobate ($KNaNbO_3$, KNN) seems to be the most promising as its structure resembles that of PZT owing to which it shows comparatively higher dielectric and piezoelectric properties [1]. However, it's highly volatile nature leads to poor densification of the ceramics; thus, high d_{33} values cannot be attained. In order to produce well densified KNN ceramics, various modifiers and sintering aids such as Ba, Bi, Li, Ta, Sb, ZnO, $SrTiO_3$, MnO_2, *etc.* have been added to the KNN composition [2–10]. Of all these, Li and Sb have proved to be most promising as KNN modified with Li and Sb possesses high piezoelectric and dielectric properties [11, 12]. Modifying KNN with Li has been reported to enhance the Curie temperature (T_c) [13, 14] whereas modifying KNN with Sb reduces it [15], so the optimum T_c can be obtained if we modify the KNN system with both Li and Sb. In previous works, high d_{33} values were obtained in KNN-LS systems [16–18].

*E-mail: gaur.roopam@gmail.com
†E-mail: kongbam@gmail.com
‡E-mail: l_radhapiyari@hotmail.com

Achieving a high density and optimum properties simultaneously is still a task to be achieved. Various sintering methodologies, such as Spark Plasma sintering (SPS) and hot (HIP) and cold (CIP) isostatic pressing have been used in order to achieve these [19–21]. However, all these processes are very expensive and cannot be used on an industrial scale. Thus, we have to find a way to produce KNN ceramics so that they are optimally dense, possess optimal piezoelectric properties, and are industrially viable. Thus, in order to overcome problems such as poor densification, high aging rate, poor piezoelectric properties, high sintering temperatures, *etc.*, we have done a detailed study on the sintering behavior of KNLNS ceramics.

We have done so by modifying KNN with 4-mol % Li and 4-mol % Sb and synthesizing the ceramics by using a mixed oxide routine and conventional sintering technique so as to maintain the industrial viability of the ceramics prepared.

II. EXPERIMENTAL PROCEDURE

Lead-free KNLNS ceramics were synthesized by using the normal solid-state reaction method with high-purity ($> 99\%$) K_2CO_3, Na_2CO_3, Li_2CO_3 and Nb_2O_5 powders. As the alkali carbonates are extremely hygroscopic in nature, they were systematically dried at 200 °C for 2 h before using them. All these precursors were then weighed according to the desired composition, were homogenized first by ball-milling in 2-propanal for 15 h and then were ball-milled again in a Retsch PM 100 planetary high-energy ball mill for 5 h at an angular rate of 300 rpm. The obtained powders were then calcined in alumina crucibles at 900 °C for 3 h.

To assure the homogeneity in the samples prepared, we again ball-milled the calcined powders in the high-energy ball mill for an hour (with same settings as before) and then dried them in an oven for 4 h at a low temperature of 70 °C to avoid spilling of the liquid sample from the beaker. The obtained powders were then mixed with polyvinyl alcohol (binder) and granulated thoroughly in order to obtain a homogeneous mixture, and were then pressed into disks (diameter: 10 mm) using a hydraulic press. The pellets thus prepared were sintered at various temperatures ranging from 1050 °C to 1090 °C for 2 h $\sim$ 3 h. Comparative study of the piezoelectric, dielectric and microstructural properties of these ceramics was then carried out.

The densities of the sintered pellets were measured by using Archimedes' Principle. The average grain size measurement was done using the mean intercept length method from at least five different areas of the sample. The crystal structure of the sintered specimens was studied using an X-ray diffractometer (Philips Diffractometer PW 3020) with monochromatic Cu K_α radiation (λ = 1.54178 Å) over a 2θ angle from 20° to 70°. The microstructure of the fractured ceramics was studied using Scanning electron microscopy (SEM, Leo 1430, Japan). In order to perform electrical characterization, we fired silver electrodes on the pellets at 150 °C for 1 h. The ferroelectric hysteresis loops of the ceramics were measured at room temperature by using an automated *P-E* loop tracer (AR Imagetronics, India) operating at 50 Hz. Specimens for the piezoelectric measurements were poled for 30 min in a 120 °C silicone-oil bath by using a dc electric field of 3 kV/mm. The dielectric properties were measured by using a LCR meter (ANDO 4304). The piezoelectric constant d_{33} was measured using a Piezo d_{33} meter (YE2730A d_{33} METER).

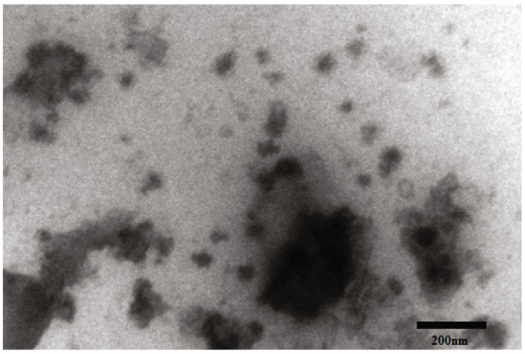

Fig. 1. Typical TEM micrograph of KNLNS nanopowders.

III. RESULTS AND DISCUSSION

The KNLNS ceramics were prepared from nanopowders with an average particle size of about 35 nm. A typical transmission electron microscopy (TEM) micrograph of the KNLNS nanopowders is shown in Fig. 1. The typical XRD patterns of the lead-free KNLNS ceramics sintered under different sintering conditions are shown in Fig. 2. The XRD patterns were indexed by using JCPDS no. 71-0946 in the ICDD database. As we can see, some extra peaks are seen for the pellets sintered at 1050 °C and 1090 °C which proves that these temperatures are not suitable for sintering, but for sintering temperatures of 1070 °C and 1080 °C the crystal remains in single phase perovskite structure and no secondary phase is observed. The absence of any secondary phase indicates that Li^+ and Sb^{5+} have diffused very well into the KNN lattice, with Li^+ and Sb^{5+} occupying the $(Na_{0.5}K_{0.5})^+$ and the Nb^{5+} sites, respectively, to form a solid solution. No significant shifting of any kind is seen in the peaks, which could be due to the facts that all four compositions are same and they had been sintered at different temperatures in a very narrow range. Thus, not much change in the crystal phase structure is expected, so no evident shifting in the peaks should be displayed. The splitting of the (022) and the (200) peaks confirms the existence of orthorhombic symmetry

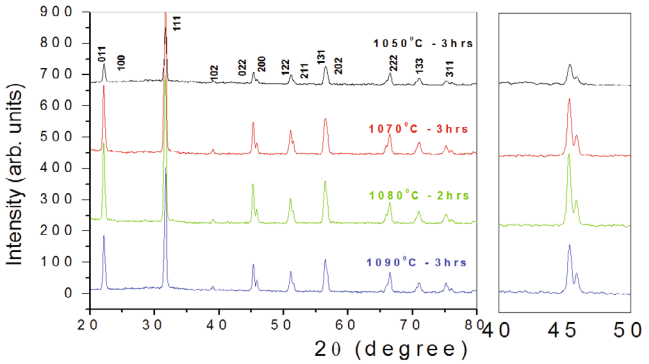

Fig. 2. (Color online) X-ray diffraction patterns of the $(K_{0.48}Na_{0.48}Li_{0.04})$ $(Nb_{0.96}Sb_{0.04})$ O_3 crystal sintered at 1050 °C (3 h), 1070 °C (3 h), 1080 °C (2 h) and 1090 °C (3 h). (a) XRD pattern for 2θ ranging from 20° to 70° (b) enlarged pattern for 2θ ranging from 44° ∼ 47°.

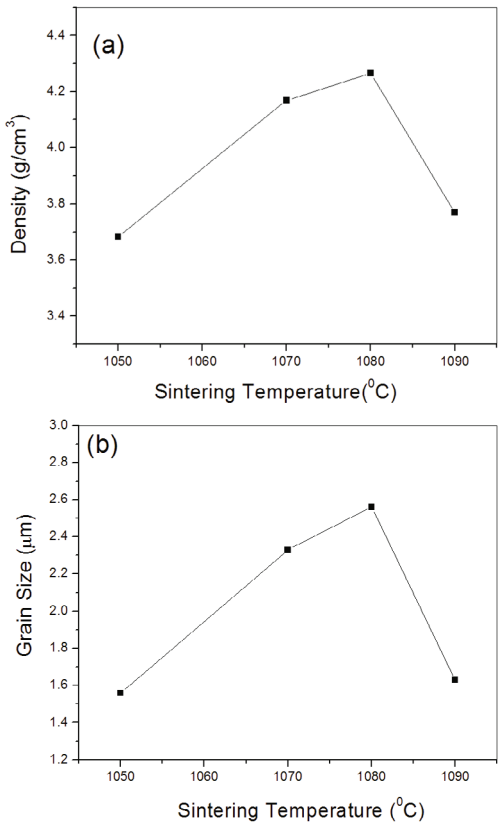

Fig. 3. (a) Density and (b) grain size variation with sintering temperature. The samples were sintered for 3 h at 1050, 1070 and 1090 °C and for 2 h at 1080 °C.

at room temperature. These results coincide with those of earlier works that reported orthorhombic symmetry for ceramics of similar compositions [16].

Moving on to the density of the ceramics prepared, in Fig. 3(a), we show that the bulk density reaches its maximum for annealing at a temperature 1080 °C for a duration of 2 h. The density increases with increasing

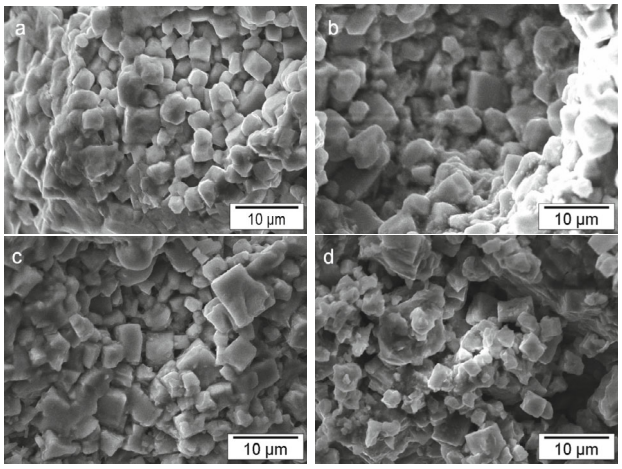

Fig. 4. SEM images of freshly fractured surfaces of KNLNS ceramics sintered under various conditions: (a) 1050 °C for 3 h, (b) 1070 °C for 3 h, (c) 1080 °C for 2 h, and (d) 1090 °C for 3 h.

the sintering temperatures up to 1080 °C, and its values are 3.683 g/cm^3, 4.169 g/cm^3 and 4.266 g/cm^3 at 1050 °C (3 h), 1070 °C (3 h) and 1080 °C (2 h), respectively. At temperatures above 1080 °C, the density decreases to 3.769 g/cm^3 when the sintering temperature is increased to 1090 °C (3 h). This may be due to an increase in the vapor pressures of elements like K^+ and Li^+, which probably leads to a decrease in the weight of the samples. The density pattern is supported by the SEM images of the fractured surfaces of the KNLNS ceramics shown in Fig. 4. With varying sintering conditions, the grain size increases gradually until the optimum sintering condition is reached. This leads to a decrease in the porosity and an increase in the compactness in the ceramics, as can be seen in Fig. 4(c). The ceramics sintered at 1050 °C for 3 h (1050 °C - 3 h) have grain size of about 1.56 μm, and the grains are mostly small with very few pores (Fig. 4(a)). When we increase the sintering temperature, an increase in the grain size occurs with undefined grain boundaries, which helps in reducing the porosities and, thus, leads to an increased density of the ceramics, (Fig. 4(b)) [18,22]. However, as we approach optimum sintering condition, grains become uniformly cubic with an average size of 2.56 μm with defined grain boundaries, giving rise to compactness in the structure, as is evident in Fig. 4(c). Now, when we further increase the sintering temperature, Fig. 4(d), the grain size decreases, which, in turn, creates increased porosities in the ceramics. The gaps between the grains reduce the net weight of the ceramics, leading to poorer density of the ceramics. The variation of grain size is shown in Fig. 3(b). As reported in previous works, an increase in grain growth takes place with a liquid phase, which, in turn, induces secondary phase [23], but in our case, the slight liquid phase that is seen when the ceramics are sintered at 1070 °C (3 h) disappears when we reach the optimum sintering condition

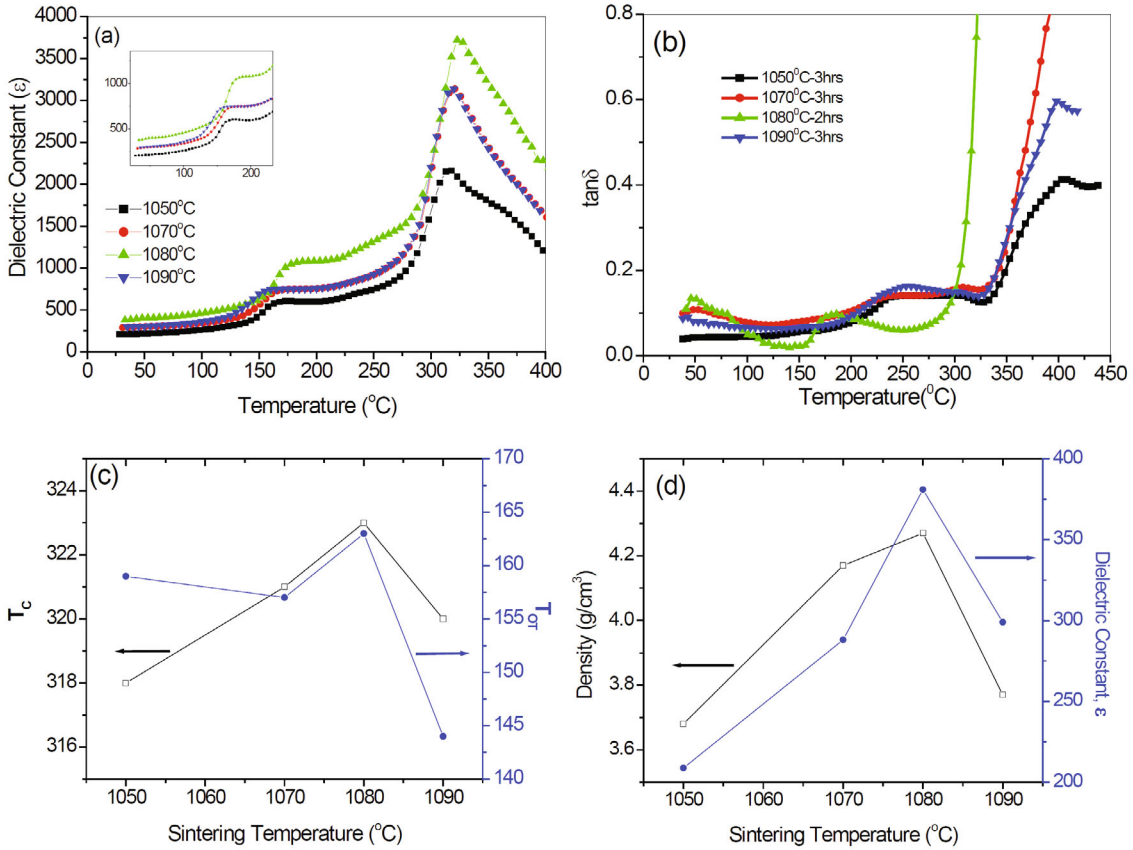

Fig. 5. (Color online) Dielectric properties of KNLNS ceramics sintered under different sintering conditions.: (a) dielectric constant vs. temperature, (b) tanδ vs. temperature, (c) T_c and T_{ot} vs. sintering temperature, and (d) density and dielectric constant vs. sintering temperature.

of 1080 °C (2 h). As seen in the XRD pattern, secondary phase developed in our work [24]. The dielectric constants of the ceramics also follow a pattern similar to those of density and grain size. Figure 5(d) shows how the dielectric constant varies with changing sintering condition. The increase in the density of the samples is responsible for the increase in the dielectric constants of the ceramics. The ceramic sintered at 1080 °C for 2 h shows the highest dielectric constant, 381, at room temperature. At temperatures beyond 1080 °C, the dielectric constant decreases owing to the decreased density. The temperature dependence of the dielectric constants for KNLNS samples sintered at temperatures of 1050 °C (3 h), 1070 °C (3 h), 1080 °C (2 h) and 1090 °C (3 h) measured at 100 kHz are shown in Fig. 5(a). Just like the pure KNN, the dielectric constant vs. temperature curves for the KNLNS ceramics also evidenced two phase transitions: *i.e.*, a tetragonal-to-cubic transition at the Curie temperature (T_c) and an orthorhombic-to-tetragonal transition at a temperature T_{ot} [25]. The T_c of the ceramics range from 318 $\sim$ 325 °C, and it shifted to higher temperatures as we approached the optimum sintering condition. Earlier, many works have reported that the partial substitution of Li^+ for $(Na\ K)^+$ ions increases the T_c whereas that of Sb^{5+} with Nb^{5+} decreases it [14, 15]. Because we did not see very high values of T_c as reported in the literatures [26], we may conclude that the effect of Sb substitution dominated the effect of Li substitution and that this may be due to the highly volatile nature of the alkali elements, which may eventually lead to their decrease in the composition while the Sb^{5+} ions, which do not experience any such problem, remain in the designated amount in the composition. Also, we can see in Fig. 5(c) that T_c first increases till 1080 °C and then decreases as we increase the temperature [27]. This may be due to the increased volatility of alkali members owing to the increase in the temperature. The orthorhombic-to-tetragonal transition temperature T_{ot} decreased gradually throughout. The T_c value reported in this paper coincides with the values in many previous works, including works that used compositions that were very similar to the ones used [16], but the values of the T_{ot} of the present ceramics were not close. The T_{ot} reported in this paper is quite high as compared to the above mentioned compositions. Morphotropic Phase Boundaries (MPBs) are found when the T_{ot} temperature shifts to lower values and ultimately reaches room temperature. Due to this, we obtain the tetragonal and the

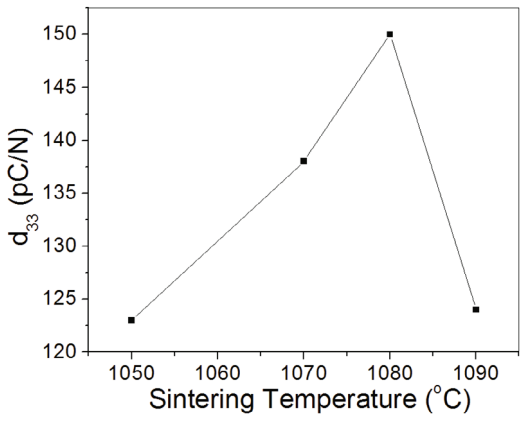

Fig. 6. Piezoelectric properties of KNLNS ceramics.

Table 1. Dielectric, microstructural and piezoelectric properties of KNLNS ceramics.

	1050-3h	1070-3h	1080-2h	1090-3h
Density (g/cm^3)	3.68	4.17	4.27	3.77
Grain size (μm)	1.56	2.33	2.56	1.63
Dielectric (const)	209	288	381	299
T_c (°C)	318	321	323	320
T_{ot} (°C)	159	157	163	144
$\tan\delta$	0.039	0.099	0.109	0.08
d_{33} (pC/N)	123	138	150	124

orthorhombic symmetries simultaneously at room temperature, and this gives rise to enhanced properties of the ceramics prepared. However, in this work, the T_{ot} values are quite high and nowhere close to room temperature. Thus, all the ceramics prepared in this work are in absolute orthorhombic symmetry at room temperature, and because most of the characterizations took place at this temperature only, the properties we report are those of ceramics in orthorhombic symmetry. The high T_{ot} values could be due to the presence of a higher percentage of Sb^{5+} compared to Li^+, unlike in previous works. However, still we have obtained transition temperatures for these ceramics that are lower than that of pure KNN, yet we obtain the same XRD pattern, which proves that Li^+ and Sb^{5+} have been absorbed by the KNN matrix. Figure 5(b) shows the dependence of the dielectric loss of KNLNS ceramics on the sintering conditions. As can be seen in the figure, it first decreases with increasing temperature and then increases exponentially [28]. The sudden rise of the dielectric loss factor at higher temperatures could be attributed to the increased mobility of the charge carriers in the ceramics, which increases the conductivity.

According to Fig. 6, the piezoelectric charge coefficient d_{33} also shows a peak at 1080 °C (2 h). This increase and decrease in the d_{33}, is attributed to the density of the ceramics prepared. The highest d_{33} value was obtained for the ceramic with the highest density and dielectric constant.

IV. CONCLUSION

A dense microstructure is obtained under optimum sintering conditions without any secondary phase. The grain growth helps in increasing the compactness of the grains, thus promoting densification in the ceramics. The properties of ceramics sintered at 1080 °C for 2 h are T_c = 323 °C, ε_{RT} = 381, ε_{max} = 3723, d_{33} = 150 pC/N, density = 4.26 g/cm^3, grain size = 2.56 μm. Hence, we conclude that, for KNN modified with Li and Sb, the optimum temperature and duration for sintering are 1080 °C and 2 h. We can achieve very good electrical and piezoelectric properties by using a conventional sintering method without using any sintering aid. The composition showed no secondary phases, which improved the stability of the ceramics. Hence, we suggest that Li- and Sb-modified KNN ceramics are good candidates for lead-free piezoceramics and that they are great subjects for further studies.

ACKNOWLEDGMENTS

The authors acknowledge the financial support from the Department of Science and Technology, India, under the Research project no. SR/S2/CMP-0017/2011.

REFERENCES

[1] L. Egerton and D. M. Dillon, J. Am. Ceram. Soc. **42**, 438 (1959).
[2] S. H. Choy and H. L. W. Chan, Curr. Appl. Phys. **11**, 869 (2011).
[3] E. Hollenstein, M. Davis, D. Damjanovic and N. Setter, Appl. Phys. Lett. **87**, 182905 (2005).
[4] S. T. F. Lee, K. H. Lam, X. M. Zhang and H. L. W. Chan, Ultrasonics **5**, 811 (2011).
[5] J. B. Lim, S. Zhang, J. Jeon and T. R. Shrout, J. Amer. Soc. **93**, 1218 (2010).
[6] F. Rubio-Marcos, J. J. Romero, M. G. Navarro- Rojero and J. F. Fernandez, J. Eur. Ceram. Soc. **29**, 3045 (2009).
[7] S. C. Ur, I. Mahmud and M. S. Yoon, Ceram. Inter. **39**, 691 (2013).
[8] H. Wang, H. Zhai, J. Xu, C. Yuan and C. Zhou, J. Mater. Sci. **24**, 2469 (2013).
[9] H. Xinyou, G. Chunhua, C. Zhigang and J. Huiping, J. Rare Earths **24**, 321 (2006).
[10] R. Zuo, J. Fu, X. Wang and L. Li, J. Mater. Sci. **21**, 519 (2010).
[11] H. E. Mgbemere, R. P. Herber and G. A. Schneider, J. Eur. Ceram. Soc. **29**, 3273 (2009).

[12] S. Zhang, R. Xia, T. R. Shrout, G. Zang and J. Wang, Solid State Commun. **141**, 675 (2007).
[13] J. Wang Wu, D. Xiao, Y. Wang, J. Zhu, P. Yu and Y. Jiang, J. Appl. Phys. **102**, 114113 (2007).
[14] M. Matsubara, T. Yamaguchi, K. Kikuta and S. Hirano, Jpn. J. Appl. Phys. **44**, 6136 (2005).
[15] H. E. Mgbemere, G. A. Schneider and T. A. Stegk, Func. Mater. Lett. **3**, 25 (2010).
[16] R. Rani, S. Sharma, R. Rai and A. L. Kholkin, Solid State Sci. **17**, 46 (2013).
[17] J. Wu, D. Xiao, Y. Wang, J. Zhu, P. Yu and Y. Jiang, J. Appl. Phys. **102**, 114113 (2007).
[18] Y. Zhao, R. Huang, R. Liu, X. Wang and H. Zhou, Ceram. Inter. **39**, 425 (2013).
[19] R. E. Jaeger and L. Egerton, J. Am. Ceram. Soc. **45**, 209 (1962).
[20] G. H. Haertling, J. Am. Ceram. Soc. **50**, 329 (1967).
[21] L. Egerton and C. A. Bieling, Ceramic. Bull. **47**, 1151 (1968).
[22] D. Lin, K. W. Kwok, K. H. Lam and H. L. W. Chan, J. Phys. D: Appl. Phys. **40**, 3500 (2007).
[23] S. H. Park, C. W. Ahn, S. Nahm and J. S. Song, Jpn. J. Appl, Phys. **43**, L1072 (2004).
[24] F. Rubio-Marcos, J. J. Romero, M. S. Matrin Gonzalez and J. F. Fernandez, J. Eur. Ceram. Soc. **30**, 2763 (2010).
[25] I. Smeltere, M. Antonova, A. Kalvane, O. Grigs and M. Livinsh, Mater. Sci. **17**, 62 (2011).
[26] Y. Guo, K. Kakimoto and H. Ohsato, Appl. Phys. Lett. **85**, 4121 (2004).
[27] P. K.Palei and P. Kumar, Jpn. J. Appl. Phys. **51**, 011503 (2012).
[28] B. Ming, J. Wang, P. Qi and G. Zang, J. Appl. Phys. **101**, 054103 (2007) .